Supplementary information

HS-regulation of miR824/AGL16 module does not affect stomata conductance and photosynthetic activity

miR824/AGL16 module was reported to be a regulator of stomata development (Kutter et al., 2007; Yang et al., 2014). Stomata are vital structures that are required for water and carbon dioxide uptake during photosynthesis. Water evaporation through stomata cools the surface of the leaves, preventing heat-stress damage of membranes and proteins. To unravel if *AGL16* down-regulation during and following heat stress has an impact on thermo-tolerance of photosynthetic apparatus through stomata complexity regulation we measured stomatal conductance (gs), CO_2 assimilation (Pn) and transpiration (E) rates of NT and ACCx3 plants (Col-0, *agl16-1*, Δ*824* and *MIM824*) at both 25 °C and 37 °C (Fig S9). In addition, the thermo-tolerance of the photosynthetic apparatus PS II was also investigated (Fig S9). The CO_2 assimilation activity (Pn) was lower while stomatal conductance (gs) and transpiration rate (E) were higher at 37 °C than at 25 °C (Fig S9) in leaves of both NT and ACCx3 plants. Acclimation treatment (NT vs. ACCx3 plants) modified the gas exchange parameters (Pn, gs, and E) and enhanced the thermo-tolerance of PSII as demonstrated by the temperature-dependent changes of effective quantum yield of PS II parameter (Y(II))(Fig S9A and S10). Genotypic variations were found for gs and Y(II), but no significant changes could be observed in Pn and E parameters between the different genotype groups. Since these changes did not show consistent trends, the results can't prove evidently that the temperature-dependent changes of the photosynthetic function are related to the *miR824*/AGL16 module (Fig S11). In accordance with these, we could not find differences in survival rate following different HS regimes. All these results suggest that *miR824*/AGL16 module might affect indirectly the thermo-tolerance.

Validation of agl16-1 mutant by RNA-seq

We detected an *AGL16* signal in *agl16-1* by the northern blot analysis (Fig 2A and Fig 5B). To make sure this is a specific signal, we confirmed *agl16-1* mutation by genotyping (Fig S2A), by testing the levels of *AGL16* in a qRT-PCR reaction (primers are spanning on the two sides of the SALK insertion)(Fig 2C and 5C) and a physiological assay (changes in FT, Fig 5D). *agl16-1* T-DNA insertion is located in

the last exon of *AGL16* (Fig S2B). We reasoned that a combined *AGL16*-T-DNA fused transcript is detected during northern hybridizations. Of note, *AGL16* signal in *agl16-1* is also depleted during heat similarly to the *bona fide AGL16* in wild-type Col-0 (Fig 2). To verify this possibility we analyzed RNA transcriptome data of *agl16-1* mutant and Col-0 wild-type plants (Fig S2B)(SRP151884). Comparable (slightly lower) read numbers were mapped along the *AGL16* exons in *agl16-1* (compared to Col-0 control) except for the last exon: here, at the place of T-DNA insertion, read numbers abruptly dropped. This confirms that the *AGL16* northern blot signal in *agl16-1* is specific (Fig 2 and 5). This *AGL16-T-DNA* transcript has a lower abundance and may translate a non-functional or at least hypo-functional protein.

Primer Table

Geno-typing	*lb1_sail*	gcc ttt tca gaa atg gat aaa tag cct tgc ttc c	
	lbb1_salk	gcg tgg acc gct tgc tgc aac t	
	p745_wisc	aac gtc cgc aat gtg tta tta agt tgt c	
	hsfa1a-5	aag aag ata agc cgg aga aaa tct	
	hsfa1a-6	aca aag ttg caa ccg tac tac tga	
	hsfa1b-5	cca gct tcg tca gac agt taa ata	
	hsfa1b-6	tag gaa act gtc agg att gtt tga	
	hsfa1d-5	gca taa taa ttt ctc cag ctt cgt	
	hsfa1d-6	agg ttt tcg cct agt tat tga ttg	
	hsfa1e-5	ttt taa gag gcc aaa agc aaa tac	
	hsfa1e-6	gtt gat tct tgc tcc aca cat tac	
	hsfa2_glp	aaggttccgaaccaagaaaac	
	hsfa2_grp	ctcaacaactctccttccacg	
	hsfa3_glp	aaa aga taa atc cac ggt ggc	
	hsfa3_grp	agc aag ttt ggt tgg att gtg	
	hsfa6a_glp	tca ctc aac acg aaa ccc ttc	
	hsfa6a_grp	ttc act aca acg tgt cat ggg	
	hsfa6b_glp	gtt ttg tcc gcc agc tca aca c	
	hsfa6b_grp	cct tag gct gtc cat ctc tcc	
	hsfa7a_glp	tgg agg gtt tac acg aaa atg	
	hsfa7a_grp	agc cag aaa cga cat cat ttg	
	hsfa7b_glp	ttc ttc gca agt tct gga aac	
	hsfa7b_grp	tcc cat ttt ata aga ttt tca agc	
	agl16-1_glp	acc tcc aca aga aag taa acc taa tgc	
	agl16-1_grp	cgg ttg gct gag ctg aag at	

	xrn4-6_glp	aggtgtatgctcttggcaatg	
	xrn4-6_grp	aactgccatgaaaactgatgg	
	ski2-2_glp	actcggaatcgttctgaagg	
	ski2-2_grp	tcccatcctcgagtaggcgc	
	fri_glp	ttgataaggatgagtggttcga	
	fri_grp	tgtcaacaaaaggaaccacctt	
Cloning	*prom824_F-2841*	atatgaattcacggtctgatgcgatgatcc	
	prom824_R102	atatccatgg gtcggaaaaagccgtgatgtg	
	p824HSE1m_F	gtattatcaaatcttttgtgctagcacctc	
	p824HSE1m_R	tatttaaagtttaagaggtgctagcacaaa	
	p824HSE2m_F	cgtgtggtccttaaaataataaccagcg	
	p824HSE2m_R	agatttcgctggttattattttaaggac	
	p824HSE3m_F	catttgtattcattaaatgagacaagta	
	p824HSE3m_R	taatttacttgtctcatttaatgaatac	
	proAGL16_F1gap	taacaatttcacacaggaaacagctatgacc atgattacgtgaaaccctgttaatctttt	
	proAGL16_R1gap	aaatgaaggagaaaaactagaaatttaccct cagatctacctgaatttctgaagcgggat	
Northern blot probe generation	*ACT2_F79*	ggctggatttgcaggagatg	
	ACT2_R823	cttgcccatcgggtaattca	
	AGL16_F742	ccg gta ggc tct acg att tct	AGL16_R3489 for Northern probe
	AGL16_R3489	cgg ttg gct gag ctg aag at	
	AGL16_F_3'FR	cgaacatgtccatcttcagc	
	AGL16_R_3'FR	aaattgatttggatgggaagc	
	PRIMIR824_F147	tcc gcc att ttc gaa att ctt	(combine with miR824-5p for genotyping, combine with miR824-3p for northern probe generation)
	MIR824A-5P	tcc ctt ctc aca aat ggt cta	
	MIR824A-3P	tct aga cca tcg atg aga agg	
	MIR159	tagagctcccttcaatccaaa	
	U6	*gctaatcttctctgtatcgttcc*	
	CSD1_F	*atggcgaaaggagttgcagttt*	
	CSD1_R	*ttagccctggagaccaatgatgc*	
	MIR398a	*tgtgttcacatgccactcctt*	
	MIR156h	gtgctctctttcttctgtca	
qrtPCR	ACT2-Fqrt	cgc tct ttc ttt cca agc tca t	
	ACT2-Rqrt	gca aat cca gcc ttc acc at	
	FLC_Fqrt	agccaagaagaccgaactca	
	FLC_Rqrt	tttgtccagcaggtgacatc	
	FT_Fqrt	ggt gga gaa gac ctc agg aac t	
	FT_Rqrt	ggt tgc tag gac ttg gaa cat c	
	BnaPP2A5_Fqrt	atctcttcatgggcgattacgttga	

	BnaPP2A5_Rqrt	agcgaactttgagtgctaccaag	
	Bna-pri824_Fqrt	ggtaaagagaaatggtgatttatagga	
	Bna-pri824_Rqrt	caaaacaataattccaaaagctga	
	AGL16_F2630	acc tcc aca aga aag taa acc taa tgc	
	uAGL16_R	cgacctctgaaacctggaat	(combine with F2630 for unspliced)
	AGL16_R3489	cggttggctgagctgaagat	(combine with F2630 for spliceed)
	PP2A_F	tcttttcatgggtgattatgttga	
	PP2A_R	aacgaactttcagtgctaccaaa	
	BnaAGL16_qF	gcaggctctacgagttctcc	
	BnaAGL16_qR	tttggcctcgctgtatctatc	
	PP2AA3_F	cctgcggtaataactgcatct	
	PP2AA3_R	cttcacttagctccaccaagca	
	RD29A_F	agg aac cac cac tca aca ca	
	RD29A_R	atc ttg ctc atg ctc att gc	
	UBC22_F	tcctcttaactgcgactcagg	
	UBC22_R	gcgaggcgtgtatacatttg	
ChIP	p824_-2841F_chipA	acggtctgatgcgatgatcc	
	p824_-2699R_chipA	ttcaaaacgtggcagggaac	
	p824_-978F_chipB	agttcgactcaactacactgctttaat	
	p824_-828R_chipB	ttttggctcgtccagtttttg	
	p824_25F_chipC	ccctctctcgcatccttcct	
	p824_105R_chipC	acagtcggaaaaagccgtga	
	p824_902F_chipD	ggtaaaaaggagctcgtggaaa	
	p824_986R_chipD	ttgccgaagaagaagaacgaa	
	p824_2891F_chipE	gagtttaaattgcatgcgtataaaaga	
	p824_986R_chipE	tcggatgcacccaaccatta	
	ACT2_chipF	tgccaatctacgagggtttc	
	ACT2_chipR	tctcttacaatttcccgctctg	

Supplementary references

Kutter C, Schob H, Stadler M, Meins F, Si-Ammour A (2007) MicroRNA-mediated regulation of stomatal development in Arabidopsis. Plant Cell **19:** 2417-2429

Yang K, Jiang M, Le J (2014) A new loss-of-function allele 28y reveals a role of ARGONAUTE1 in limiting asymmetric division of stomatal lineage ground cell. J Integr Plant Biol **56:** 539-549

Supplementary figure S1

A

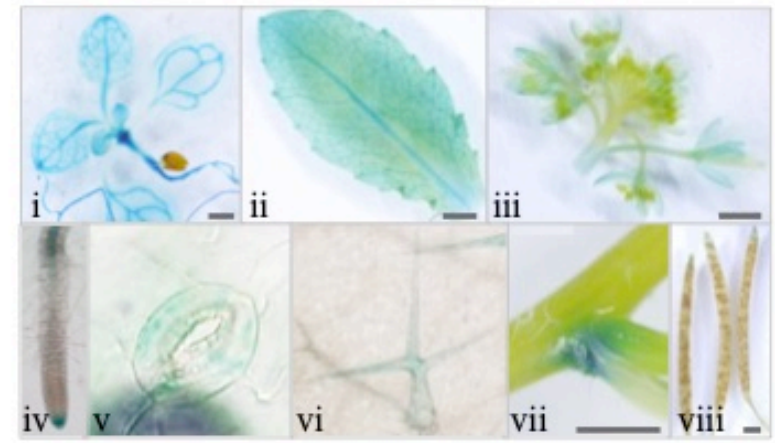

p824$_{WT}$:GUS

B

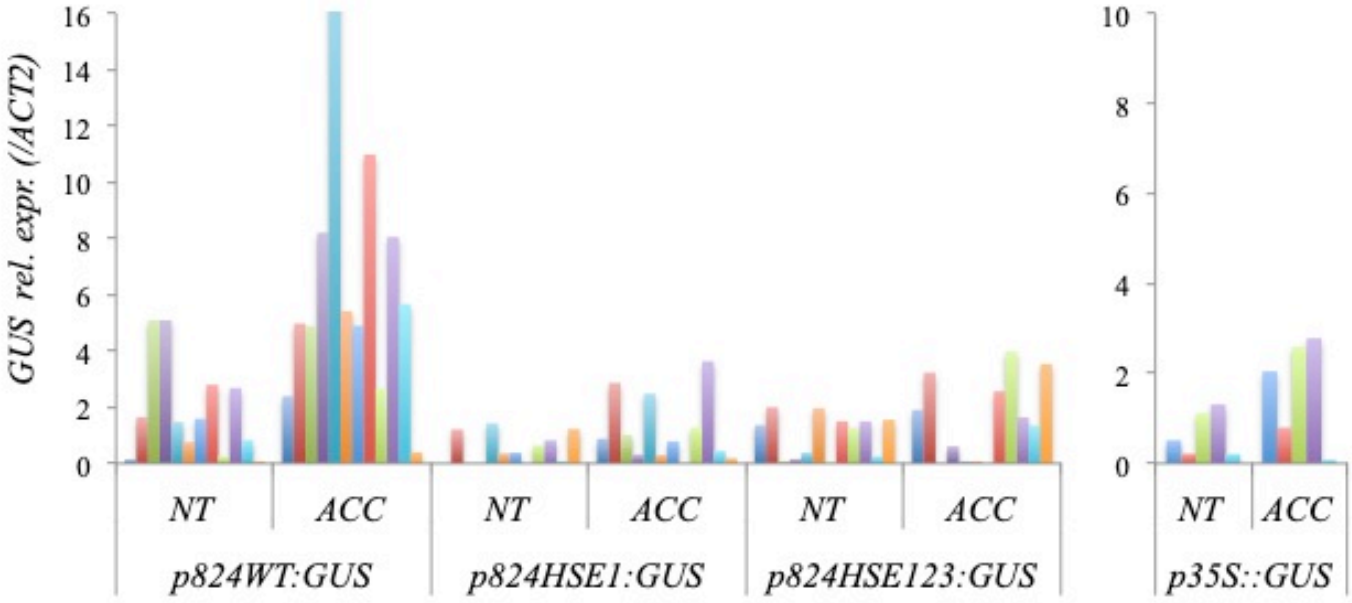

Fig S1: Heat stress induction of wild-type, single and triple mutant miR824-promoter-driven GUS transgenic lines. A. Tissue-specific activity of GUS reporter transcribed from miR824 wild-type promoter; (i) seedling; (ii) rosette leaf; (iii) inflorescence; (iv) root tip; (v) stomata; (vi) trichome; (vii) stem branching point; (viii) siliques; bars: 1 mm. **B.** *GUS* mRNA expression in independent transgenic miR824 wild-type *p824WT::GUS*, mutant *p824HSE1::GUS* and *p824HSE123::GUS* promoter lines or *p35S::GUS* control lines; the different colors represent independent transgenic lines; non-treated, NT; acclimated, ACC; *GUS* expression is relative to *ACTIN2* internal control.

Supplementary figure S2

A

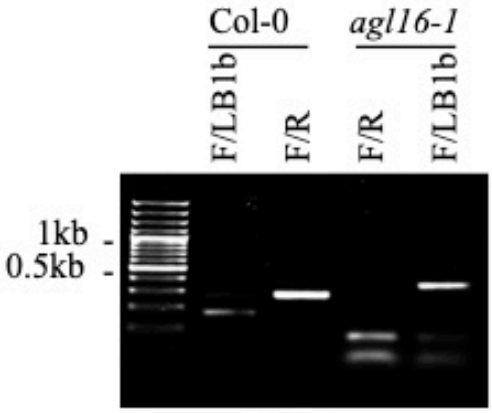

B

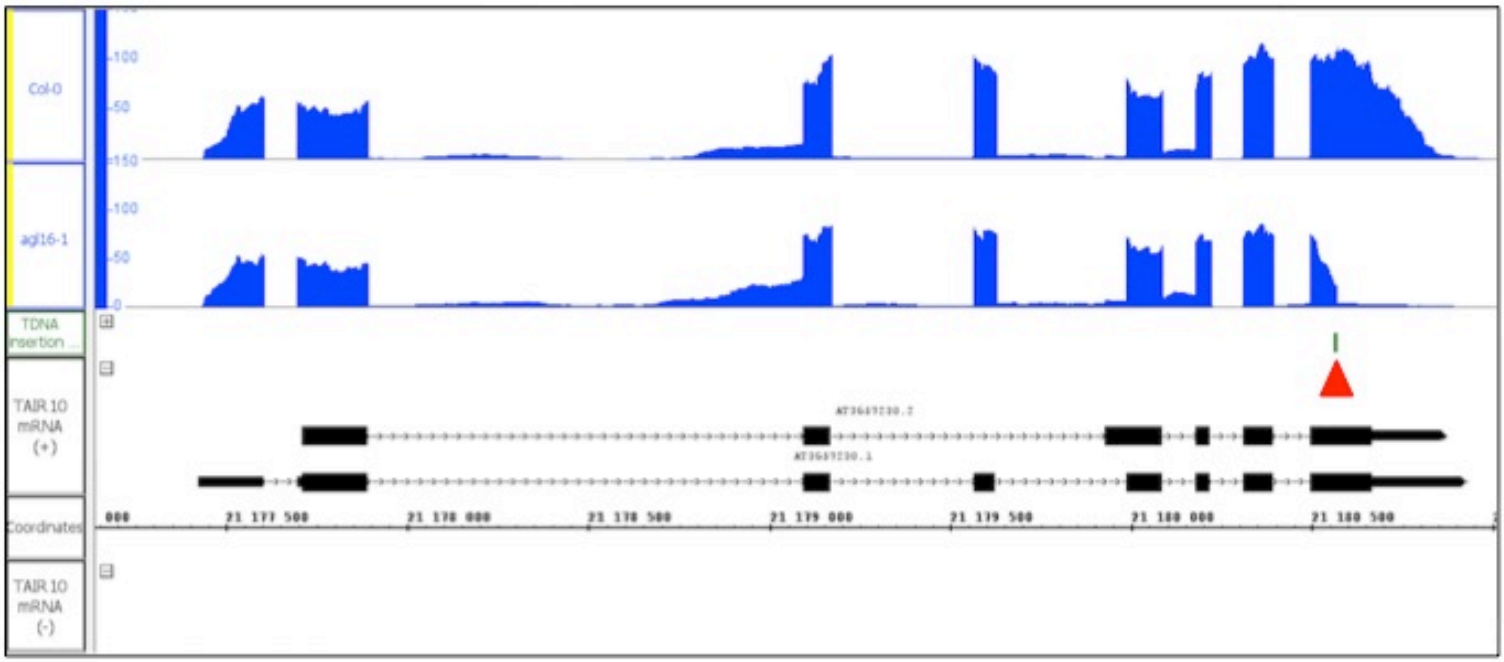

Fig S2: Confirmation of *agl16-1* (SALK_104701) T-DNA insertion within *AGL16* gene locus. **A.** PCR genotyping of *agl16-1* mutant plants and wild-type control; primers used are shown on top; size marker is shown on left. **B.** Integrated Genome Browser screenshot of *AGL16* locus presenting the RNAseq transcriptome data made from Col-0 and *agl16-1* mutant plants (blue bars, top two tracks); RNAseq read coverage of *AGL16* transcript is abruptly lost in last exon and 3'utr region at the place of T-DNA insertion (middle track, highlighted by a red triangle); *AGL16* gene locus topology is shown in the bottom track (black boxes show exons, dotted line show introns); chromosome location is shown below (black line and numbers); data are the average of 4 bio reps each.

Supplementary figure S3

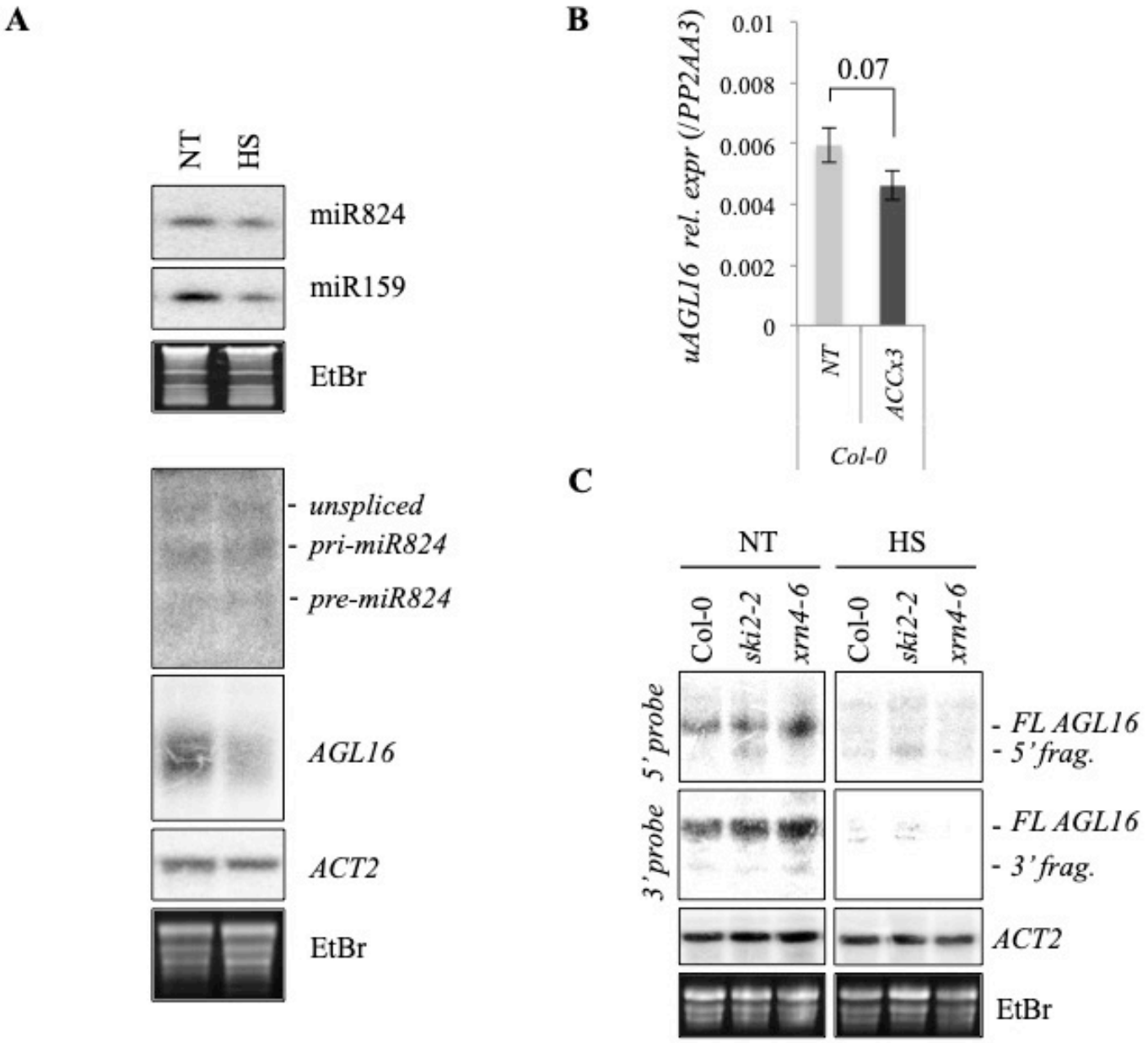

Fig S3: miR824-independent downregulation of *AGL16*. A. *AGL16* is destabilized during early heat treatment; treatment conditions are shown on top; *miR159*, *ACTIN2* and ethidium-bromid (EtBr) staining are shown as loading controls; non-treated, NT; heat-stressed, HS (45 °C/30 minutes). **B.** The level of *unspliced AGL16* (*uAGL16*) is mildly affected during heat treatment; bars represent standard error of 3 bio reps; p values based on one-tailed Student's *t*-test. **C.** Heat-induced destabilization of *AGL16* in *ski2-2* (SALK_129982) and *xrn4-6* (SALK_014209) background compared to Col-0 control; full-length (FL), 5'- and 3'- RISC cleavage fragment are indicated on right; 5' specific and 3' specific probe usage are indicated on left; miR159, *ACTIN2* and ethidium-bromide (EtBr) staining are shown as controls; non-treated, NT; heat-stressed, HS (45°C/30 minutes).

Supplementary figure S4

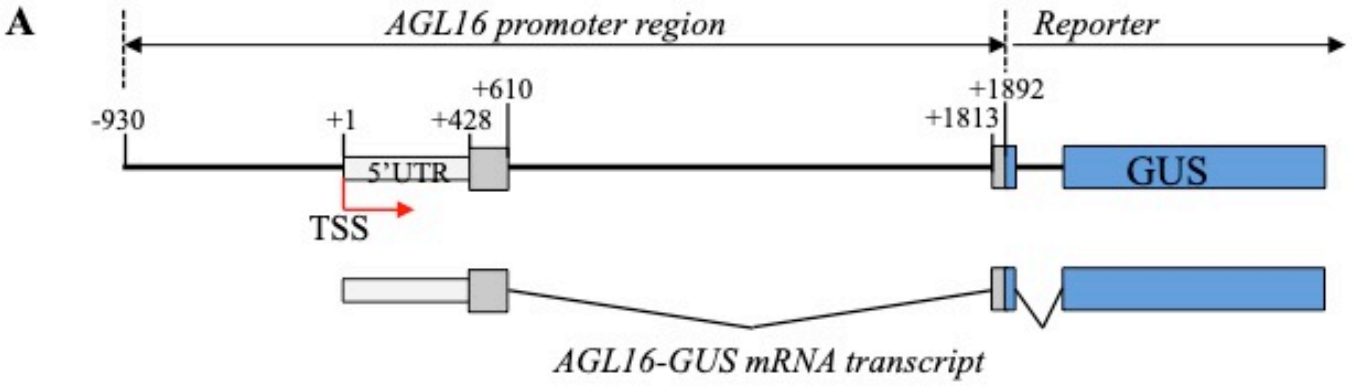

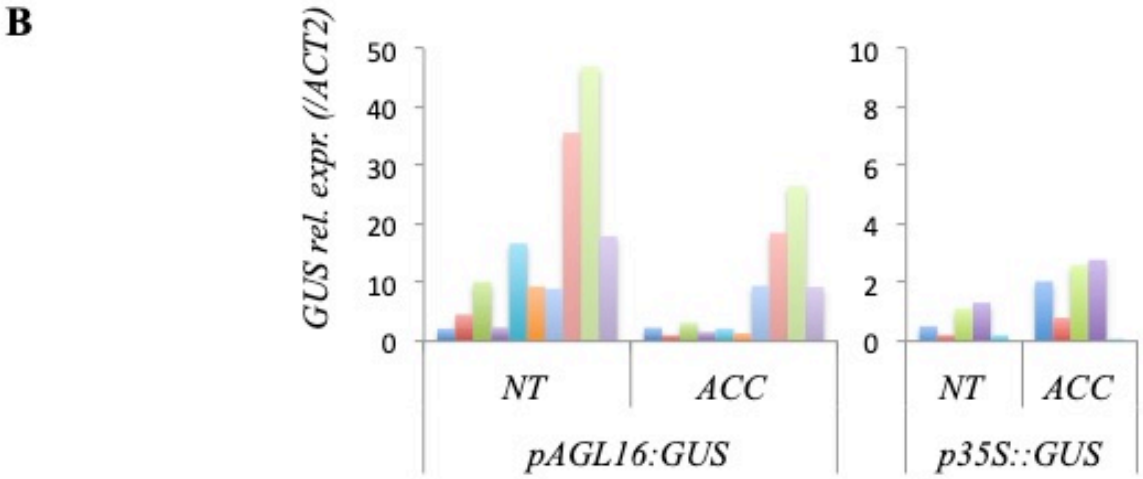

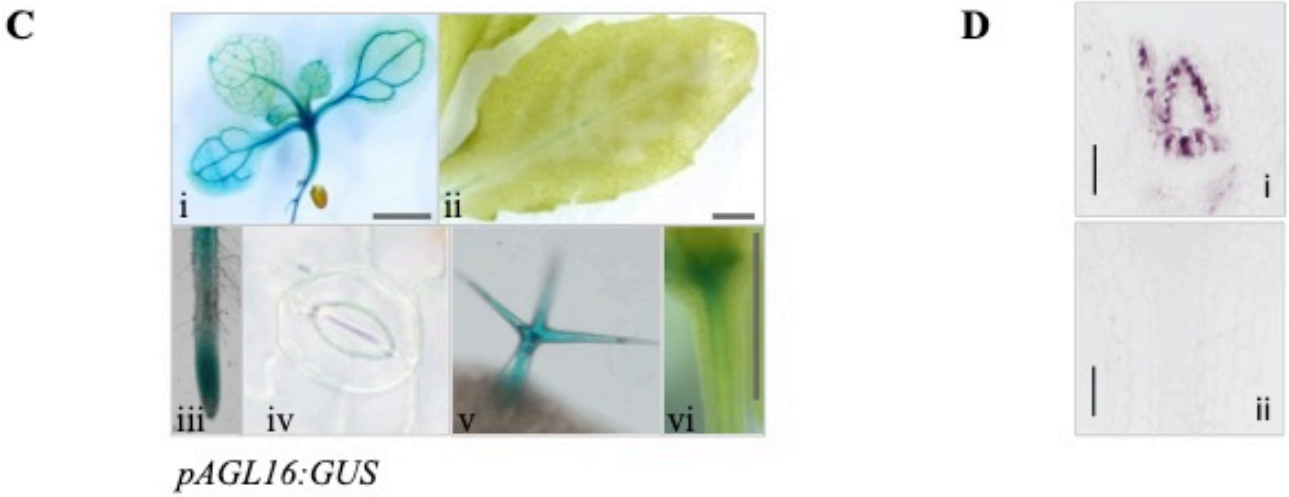

Fig S4: Tissue-specific expression and heat-induced changes of *AGL16* promoter. A. *pAGL16::GUS* reporter construct schematic representation, *AGL16* 5'UTR (light grey box), *AGL16* exons (dark grey boxes), GUS exons (blue boxes), transcription start site (TSS, red arrow), numbers denote locations relative to TSS (not to scale). **B.** Heat-induced changes in the activity of *AGL16* promoter; non-treated, NT; acclimated, ACC; *p35S::GUS* transgenic lines were used as controls; The different colors represent independent transgenic lines; Values are relative to internal *ACTIN2* control. **C.** Tissue-specific GUS staining of *pAGL16::GUS* transgenic plants: (i) seedling; (ii) rosette leaf; (iii) root tip; (iv) stomata; (v) trichome; (vi) shoot apical region; bars: 1 mm. **D.** *In situ* hybridization control using *PIN1* probe: *PIN1* mRNA is shoot apical meristem -specific (i) but not leaf vein -specific (ii); the figure is related to (Fig 5A, iv-vi).

Supplementary figure S5

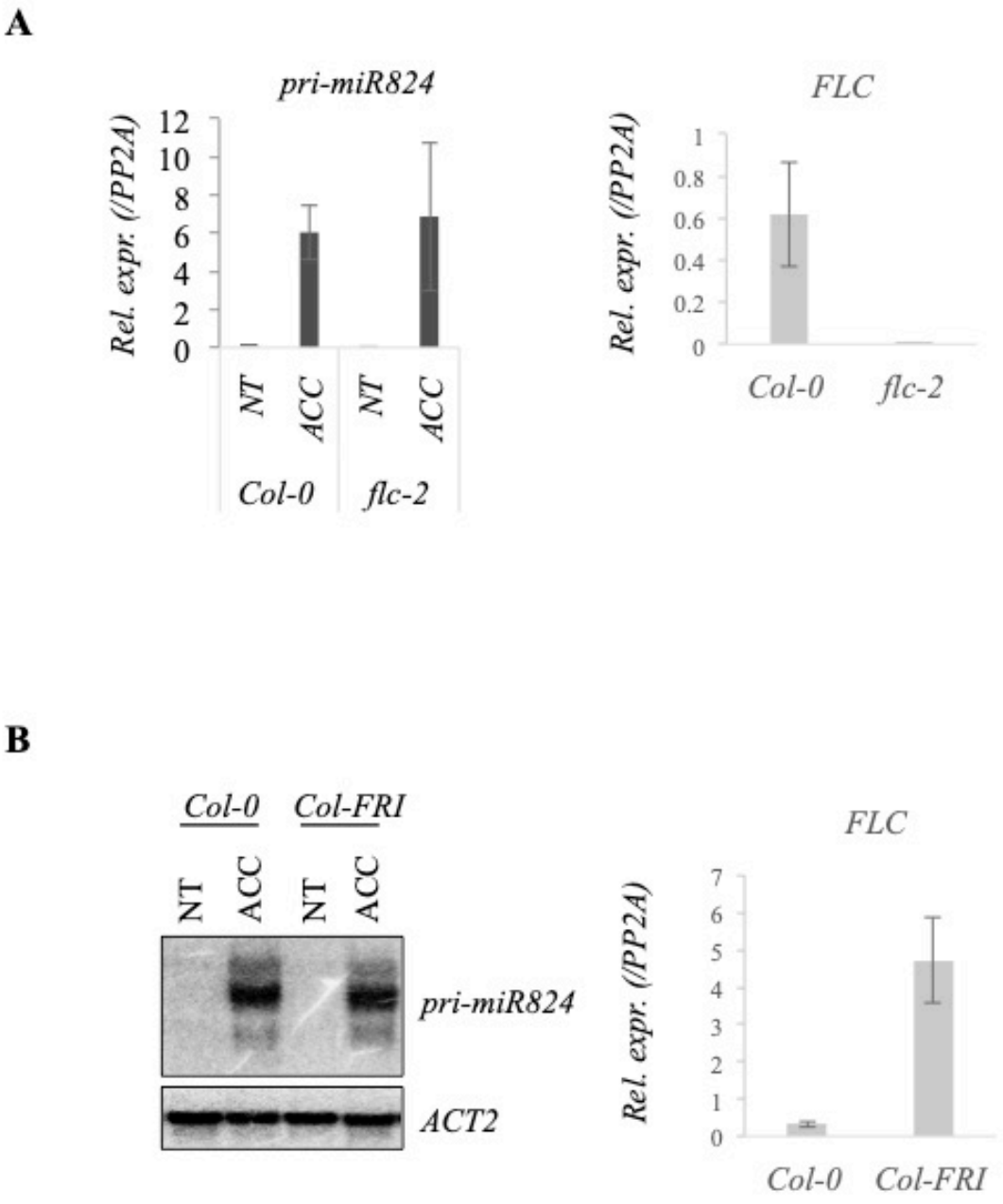

Fig S5: miR824 expression is FLC-independent. A. Basal and heat-induced expression of *pri-miR824* in Col-0 and FLC mutant *flc-2* measured by qrtPCR; *FLC* levels are shown on right as control; bars represent standard errors based on 3 bio reps. **B.** Basal and heat-induced expression of *pri-miR824* in Col-0 and Col-*FRI* background measured by northern blot. *FLC* levels measured by qrtPCR are shown on right as control; bars represent standard errors based on 3 bio reps.

Supplementary figure S6

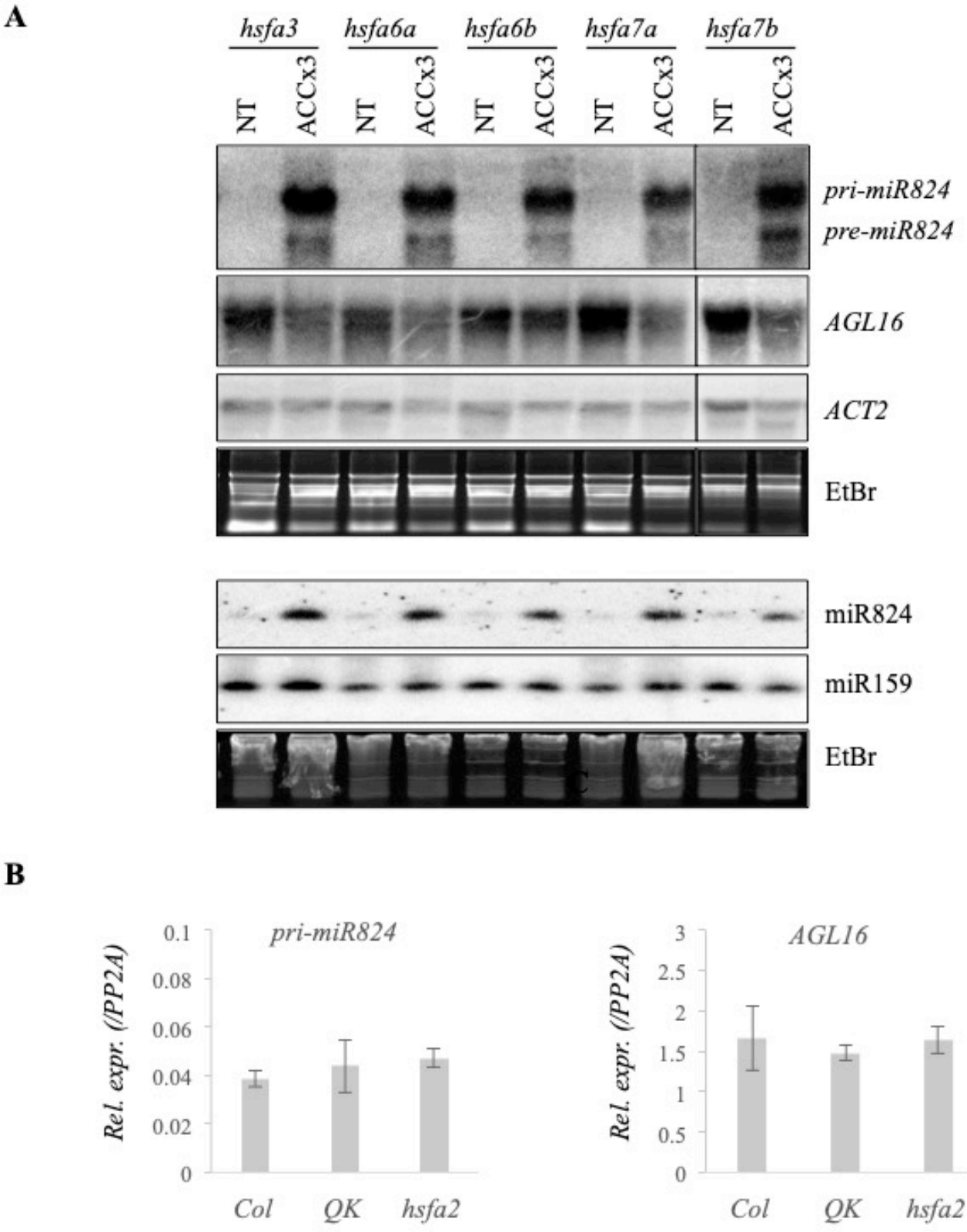

Fig S6: Heat-induction of miR824 transcription in heat shock factor mutants. A. *pri-miR824* induction and miR824 accumulation are not altered in *hsfa3*, *hsfa6a*, *hsfa6b*, *hsfa7a*, and *hsfa7b* mutants; miR159, *ACTIN2* and ethidium-bromid (EtBr) staining are shown as loading controls. **B.** Basal expression of *pri-miR824* does not depend on HSFA1a family or HSFA2 heat shock factors; *hsfa1a;hsfa1b;hsfa1d;hsfa1e* quadruple (*QK*) and *hsfa2* mutants; bars represent standard errors of 3 bio reps.

Supplementary figure S7

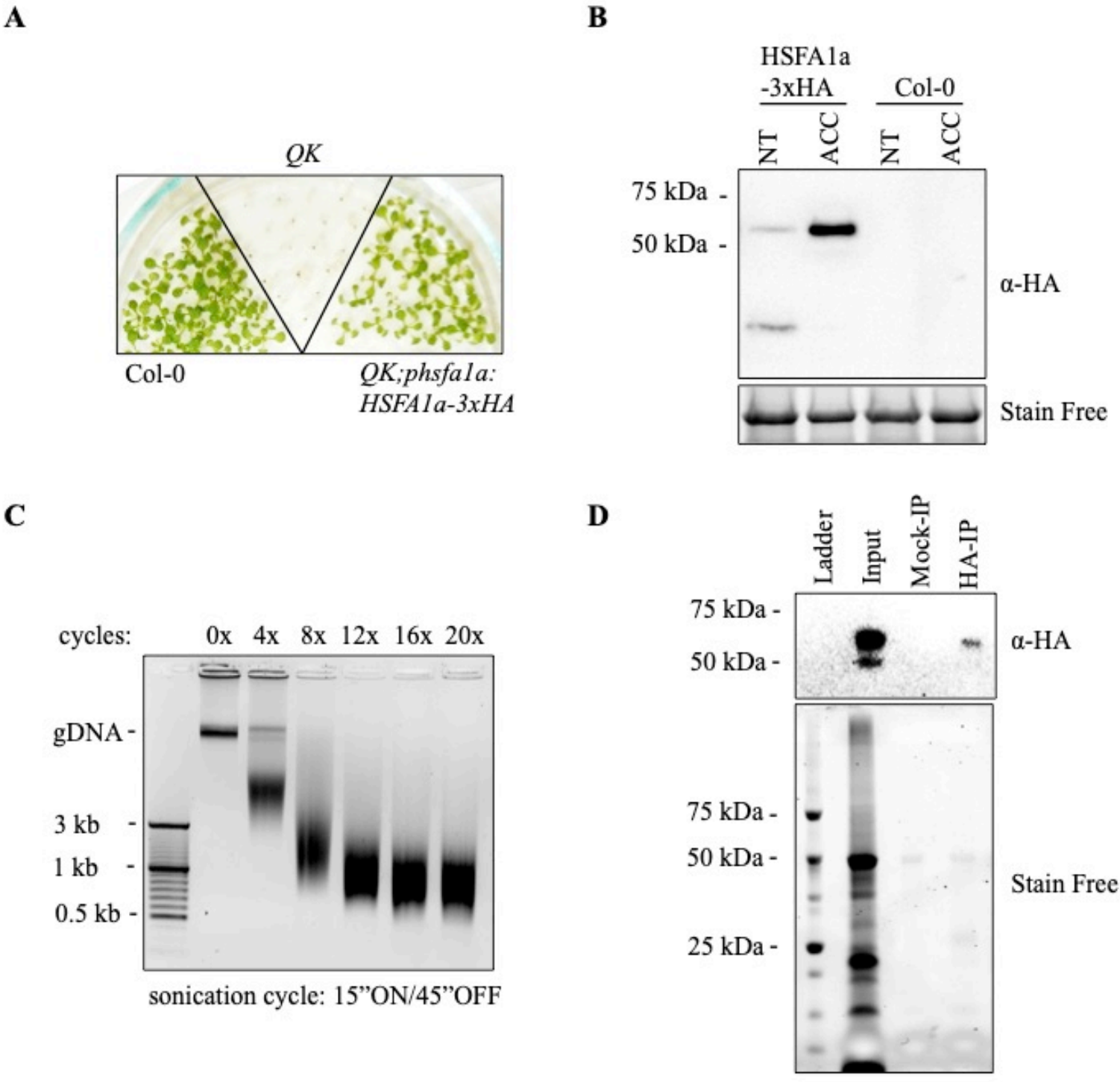

Fig S7: Chromatin immunoprecipitation using HA-tagged HsfA1a protein.
A. HSFA1a-promoter driven HA-tagged HSFA1a construct (*phsfa1a::HSFA1a-3xHA*) complements the strong phenotype of quadruple mutant *hsfa1a;hsfa1b;hsfa1d;hsfa1e (QK)* plants. **B.** HSFA1a-3xHA protein is efficiently expressed from HSFA1a own promoter during acclimation treatment; Stain-Free gel image is shown as loading control. **C.** Fragmentation of cross-linked genomic DNA following multiple rounds of sonication used for ChIP. **D.** Western blot analysis of HSFA1a-3xHA during ChIP. Stain-Free gel image is shown as a loading control; size marker is shown on the left.

Supplementary figure S8

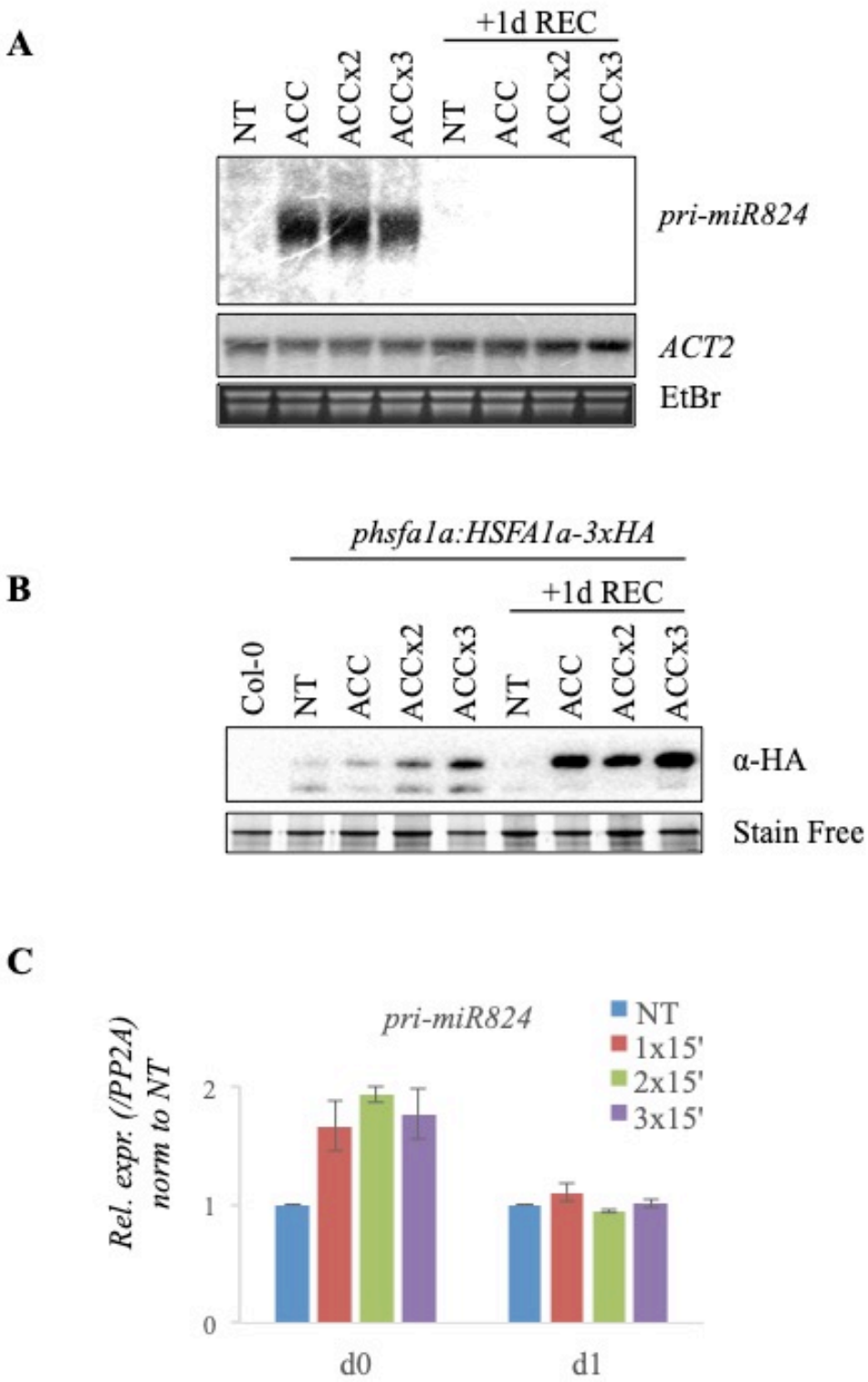

Fig S8: *MIR824* gene does not possess transcriptional memory following multiple heat-stress treatments. A. The amplitude of *pri-miR824* transcription is similar regardless of the number of acclimations and is not sustained following heat-stress. *ACTIN2* and Ethidium-bromide (EtBr) staining is shown as loading control. **B.** Western blot of HsfA1a-3xHA is showing that repeated acclimations lead to gradual accumulation of the protein; Stain Free image is shown as a loading control; samples used and treatments are shown on top. **C.** Short heat stress (37°C/15 minutes each) activate *pri-miR824* transcription to similar rate regardless of the number of treatments; qrtPCR measurements; expression values were normalized to non-treated (NT) control; bars represent standard errors of 3 bio reps.

Supplementary figure S9

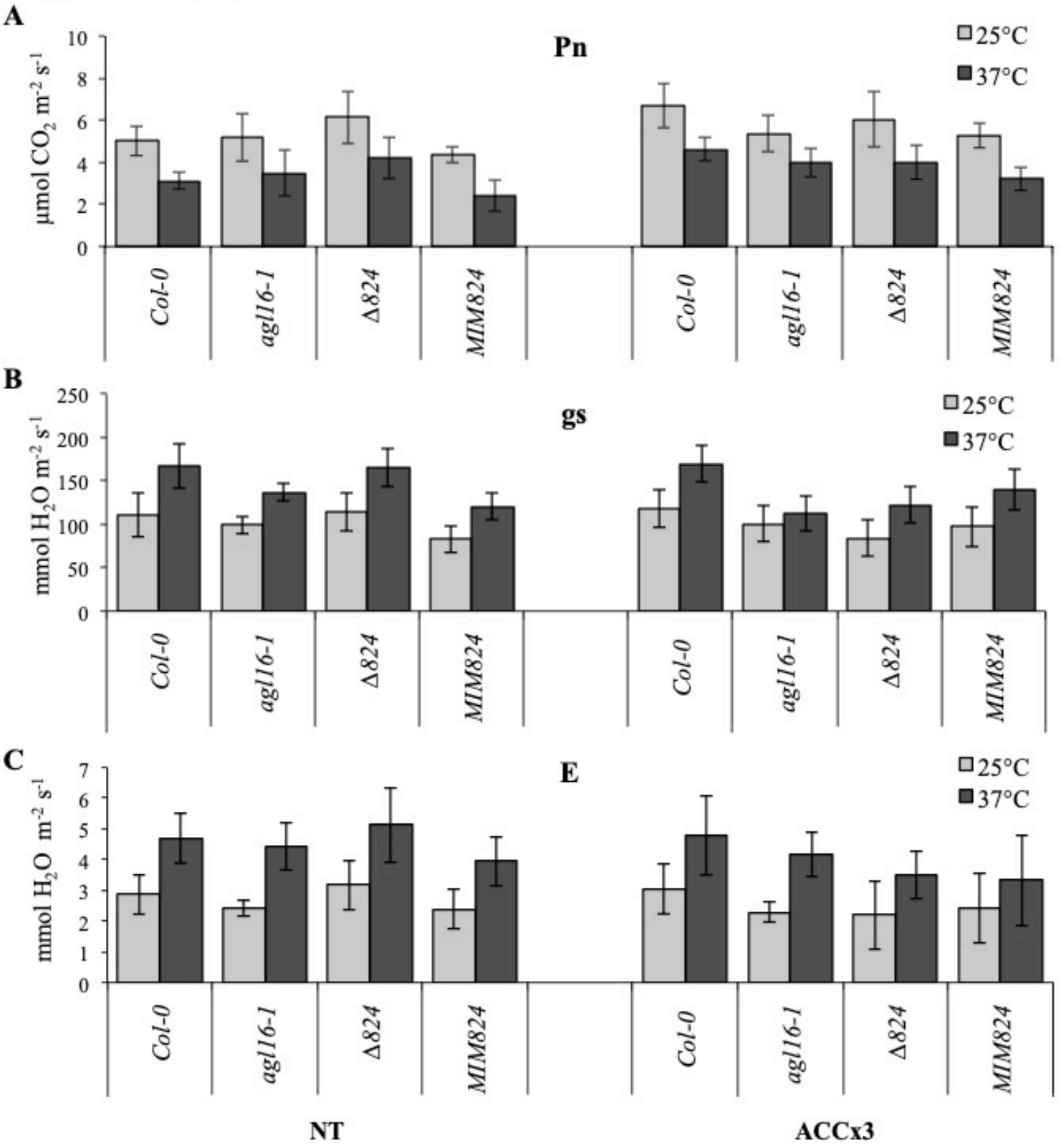

Fig S9: miR824/AGL16 module does affect heat stress response through stomata complexity changes. A. The net assimilation rate (Pn), **B.** stomatal conductance (gs) and **C.** transpiration rate (E) were determined at 25 °C and 37 °C in the non-treated (NT) and acclimated (ACCx3) mutants compared to wild-type Col-0. Bars represent the mean ± standard deviation of 6 independent measurements originated from different plants in each genotype and treatment. The results are statistically analyzed by using the General Linear Model (GLM) procedure with SPSS 23.0 software for Windows and presented in Supplementary Figure S11.

Supplementary figure S10

A

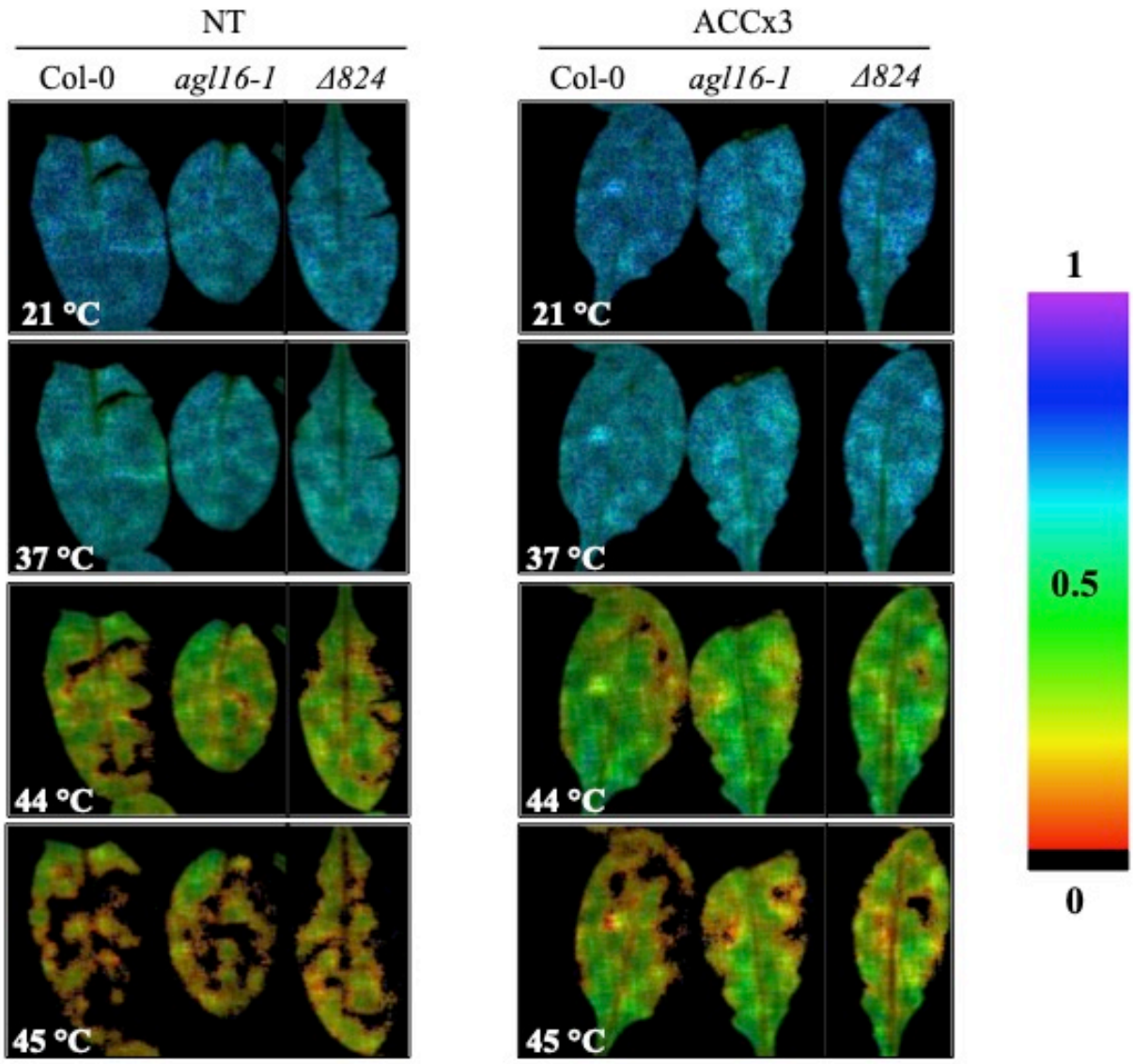

B

	NT			ACCx3		
	Col-0	agl16-1	Δ824	Col-0	agl16-1	Δ824
21 °C	0.611 ±0.020	0.590 ±0.018	0.600 ±0.020	0.626 ±0.014	0.600 ±0.017	0.621 ±0.022
37 °C	0.586 ±0.020	0.584 ±0.013	0.5769 ±0.016	0.606 ±0.013	0.595 ±0.018	0.610 ±0.018
44 °C	0.199 ±0.036	0.268 ±0.039	0.238 ±0.031	0.306 ±0.044	0.332 ±0.034	0.333 ±0.020
45 °C	0.077 ±0.017	0.143 ±0.036	0.133 ±0.028	0.197 ±0.057	0.241 ±0.028	0.232 ±0.025

Fig S10: Temperature-dependent photosynthetic activity of PSII measured by chlorophyll *a* fluorescence imaging in non-treated (NT) and acclimated (ACCx3) mutants and wild-type plant. Measurements were performed on intact detached leaves as described in Supplementary materials and methods, and the actual quantum yield of PS II parameters Y(II) measured on 21 °C, 37 °C, 44 °C and 45 °C are presented. Typical leaves are shown. Data of the table represent mean ± standard deviation of 6 independent measurements originated from different plants in each genotype and treatment. The results are statistically analyzed by using the General Linear Model (GLM) procedure with SPSS 23.0 software for Windows and presented in Supplementary Figure S11.

Supplementary figure S11

Results of statistical analyses for Fig. S9 and Fig. S10 using General Linear Model (GLM) procedure with SPSS 23.0 software for Windows.

Trait	Source of variation	Sum of Squares	Mean Square	df	F	Significance
Pn	**G**enotype	3.544	1.772	2	2.384	0.101
	ACclimation	5.757	5.757	1	7.747	**0.007**
	Temperature	57.760	57.760	1	77.716	**0.000**
	G x AC	9.944	4.972	2	6.690	**0.002**
	G x T	1.282	0.641	2	0.862	0.427
	AC x T	0.014	0.014	1	0.018	0.893
	G x AC x T	0.066	0.033	2	0.045	0.956
gs	**G**enotype	10601.361	5300.681	2	13.981	**0.000**
	ACclimation	3758.445	3758.445	1	9.913	**0.003**
	Temperature	30414.001	30414.001	1	80.221	**0.000**
	G x AC	5221.963	2610.982	2	6.887	**0.002**
	G x T	2696.268	1348.134	2	3.556	**0.035**
	AC x T	863.894	863.894	1	2.279	0.136
	G x AC x T	333.248	166.624	2	0.439	0.646
E	**G**enotype	3.367	1.683	2	2.644	0.079
	ACclimation	3.718	3.718	1	5.840	**0.019**
	Temperature	57.085	57.085	1	89.663	**0.000**
	G x AC	6.917	3.459	2	5.433	**0.007**
	G x T	0.285	0.143	2	0.224	0.800
	AC x T	0.381	0.381	1	0.599	0.442
	G x AC x T	0.297	0.148	2	0.233	0.793
Y(II)	**G**enotype	0.010	0.005	2	6.401	**0.002**
	ACclimation	0.121	0.121	1	152.286	**0.000**
	Temperature	5.299	1.766	3	2217.086	**0.000**
	G x AC	0.002	0.001	2	1.534	0.220
	G x T	0.028	0.005	6	5.865	**0.000**
	AC x T	0.058	0.019	3	24.093	**0.000**
	G x AC x T	0.002	0.000	6	0.450	0.844

Fig S11: Statistical analysis for Fig S9 and S10. Significant changes are highlighted in red.

Supplementary figure S12

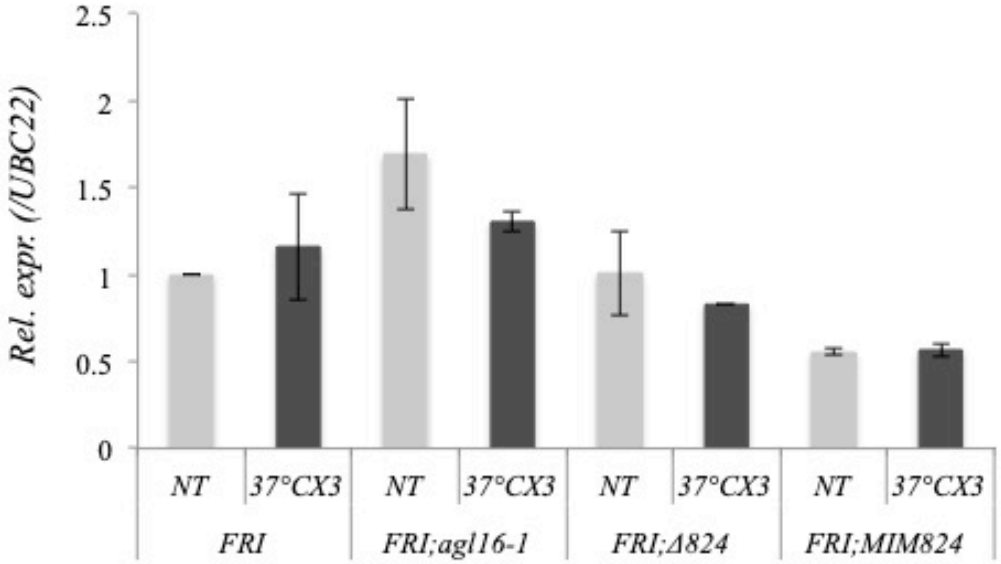

Fig S12: *FT* changes in response to repeated mild HS in wild-type and mutant plants; *UBC22* mRNA transcript was used as internal control; bars represent standard errors based on 3 bio reps.

Supplementary figure S13

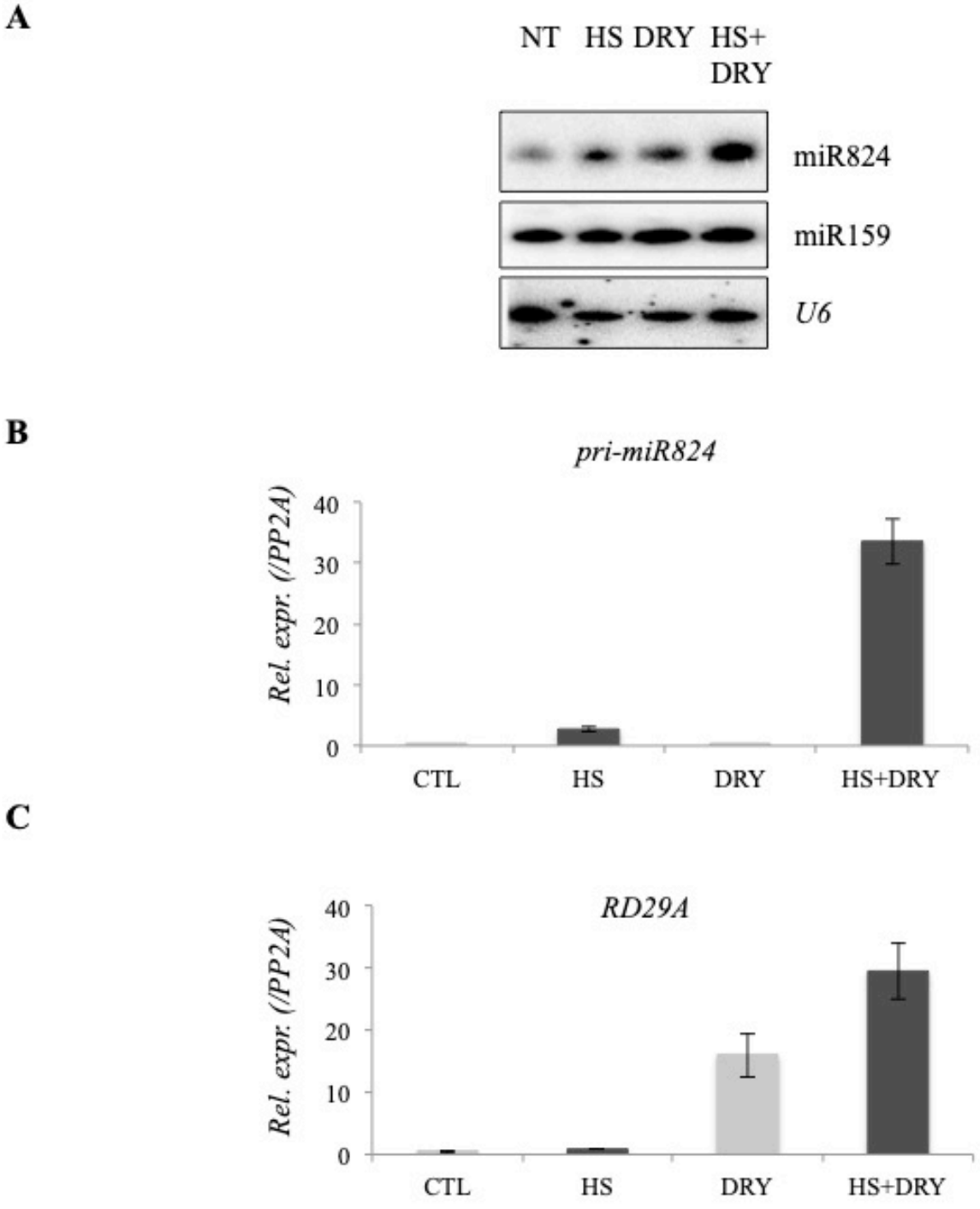

Fig S13: miR824 is strongly induced during combined heat and drought stress conditions. A. miR824 accumulation in response to heat, drought, and combined stress conditions, **B.** Relative expression levels of *pri-miR824* during diverse stress conditions; **C.** drought-induced *RD29A* mRNA changes are shown as positive control (bottom); bars represent standard errors of 3 bio reps. For drought stress, we scattered seeds on Jiffy-7® (44 mm) pellets and maintained water content on 100% of field capacity for 10 days. After 10 days we let the soil dry until water content reached 5-10% of field capacity (cca. 14 days post-germination), and collected non-treated (NT), drought-treated (DRY), heat-treated (1h 45°C) and combined stress (HS+DRY) samples.

Supplementary figure S14

A

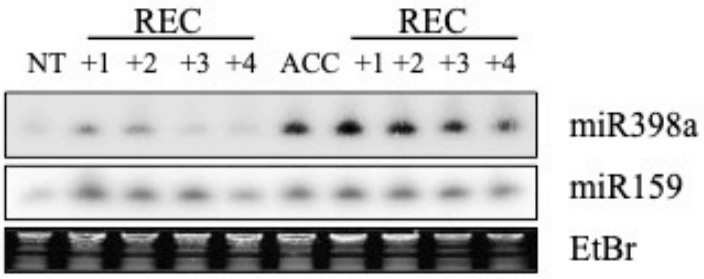

B

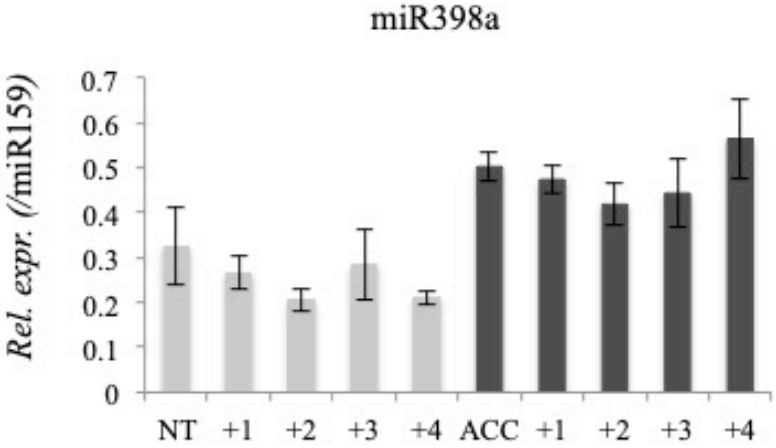

C

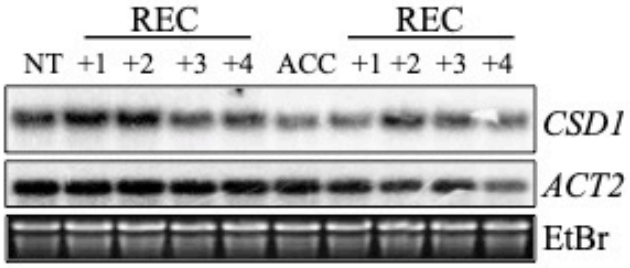

Fig S14: High level of miR398a is sustained for several days following a single heat-stress. A. Levels of miR398a level during a time-course following a single treatment (ACC) or non-treated control (NT)(treatments are shown on the top: +1, +2, +3, +4 denote days passed after the treatment); miR159 and ethidium-bromide (EtBr) staining are shown as loading controls. **B.** Quantification of miR398a northern blot measurements; Bars represent standard errors of at least 3 bio reps; **C.** *COPPER/ZINC SUPEROXIDE DISMUTASE 1* (*CSD1*) target mRNA changes during the time-course as shown in (**A.**); northern blot membranes used in (Fig 3) were re-probed with miR398a and *CSD1* probes; bars represent standard errors of 3 bio reps.